OPEN

Citation: Cell Death and Disease (2013) 4, e659; doi:10.1038/cddis.2013.193

www.nature.com/cddis

miR-129 promotes apoptosis and enhances chemosensitivity to 5-fluorouracil in colorectal cancer

M Karaayvaz[1], H Zhai[1] and J Ju*,[1]

Resistance to fluoropyrimidine-based chemotherapy is the major reason for the failure of advanced colorectal cancer (CRC) treatment. The lack of ability of tumor cells to undergo apoptosis after genotoxic stress is the key contributor to this intrinsic mechanism. Mounting evidence has demonstrated that non-coding microRNAs (miRNAs) are crucial regulators of gene expression, in particular, under acute genotoxic stress. However, there is still limited knowledge about the role of miRNAs in apoptosis. In this study, we discovered a novel mechanism mediated by microRNA-129 (miR-129) to trigger apoptosis by suppressing a key anti-apoptotic protein, B-cell lymphoma 2 (BCL2). Ectopic expression of miR-129 promoted apoptosis, inhibited cell proliferation and caused cell-cycle arrest in CRC cells. The intrinsic apoptotic pathway triggered by miR-129 was activated by cleavage of caspase-9 and caspase-3. The expression of miR-129 was significantly downregulated in CRC tissue specimens compared with the paired normal control samples. More importantly, we demonstrated that miR-129 enhanced the cytotoxic effect of 5-fluorouracil both *in vitro* and *in vivo.* These results suggest that miR-129 has a unique potential as a tumor suppressor and a novel candidate for developing miR-129-based therapeutic strategies in CRC.
Cell Death and Disease (2013) **4,** e659; doi:10.1038/cddis.2013.193; published online 6 June 2013
Subject Category: Cancer

Colorectal cancer (CRC) is the third most common cancer-related cause of death in the United States.[1] Fluoropyrimidine-based chemotherapy (e.g., 5-fluorouracil (5-FU), S-1) has been the cornerstone of treating advanced CRC for over a half century. Extensive efforts in the past have contributed to the understanding of both molecular and cellular mechanisms of action of 5-FU, one of the most important pyrimidine antagonists.[2] A number of adjuvant strategies have also been developed to further enhance the response and survival rates.

It is well established that 5-FU targets a critical enzyme, thymidylate synthase (TS). TS catalyzes the reductive methylation of deoxyuridine monophosphate to deoxythymidine monophosphate with the reduced folate 5,10-methylenetetrahydrofolate as the methyl donor.[3] As this TS-catalyzed enzymatic reaction provides the sole intracellular *de novo* source of thymidylate, an essential precursor for DNA biosynthesis, TS has been a major target of anticancer therapy.[4]

However, despite the steady improvement of 5-FU-based treatment regimen, the patient response rate to 5-FU-based chemotherapy still remains modest, mainly due to the development of drug resistance.[5] One major resistance mechanism utilized by tumor cells is to resist drug-induced cell death through disruptions of apoptotic pathways.[6] Thus, it is essential to better understand the mechanisms of drug resistance and to discover novel strategies to further improve the effectiveness of 5-FU.

In recent years, a tremendous amount of effort has been devoted to understand the mechanisms of apoptosis and to elaborate the genes/pathways involved. It has been well established that post-transcriptional and translational controls of gene expression have key roles in the cellular mechanisms of drug resistance.[7–14] Recently, a class of non-coding RNA molecules, termed microRNAs (miRNAs), has emerged as important mediators of translational control. miRNAs negatively regulate the expression of their target genes by causing translational arrest, mRNA cleavage or a combination of the two, mostly via direct targeting of the 3′-UTRs of mRNAs.[15–17] A miRNA can target multiple mRNAs, and, conversely, an mRNA can be targeted by multiple miRNAs.[18] By targeting multiple transcripts, miRNAs regulate a wide range of biological processes, including apoptosis, differentiation and cell proliferation.[19,20] Aberrant function and expression profiles of miRNAs have been reported in many types of cancers.[21,22] However, the importance of miRNAs involved in drug resistance has only been noted in the past few years.[23]

The ability of tumor cells to escape from apoptosis is complex. One of the major contributing factors is the elevated levels of anti-apoptotic protein, B-cell lymphoma 2 (BCL2). BCL2 is a central player in apoptosis of eukaryotic cells favoring survival by inhibiting cell death.[24] Overexpression of BCL2 has been reported in many types of cancer including CRC,[25] and has been widely linked to the development of resistance against chemotherapy or radiation.

[1]Translational Research Laboratory, Department of Pathology, Stony Brook University, Stony Brook, NY, USA
*Corresponding author: J Ju, Translational Research Laboratory, Department of Pathology, Stony Brook Cancer Center, Stony Brook University School of Medicine, BST-2, L-9, Room 185, Stony Brook, New York 11794, USA. Tel: +631-444-3598; Fax: +631-444-3424; E-mail: jingfang.ju@stonybrookmedicine.edu
Keywords: miR-129; BCL2; 5-fluorouracil; colorectal cancer
Abbreviations: CRC, colorectal cancer; miRNA, microRNA; miR-129, microRNA-129; 5-FU, 5-fluorouracil; TS, thymidylate synthase; BCL2, B-cell lymphoma 2; CI, combination index; FFPE, formalin-fixed paraffin-embedded
Received 25.2.13; revised 23.4.13; accepted 6.5.13; Edited by G Ciliberto

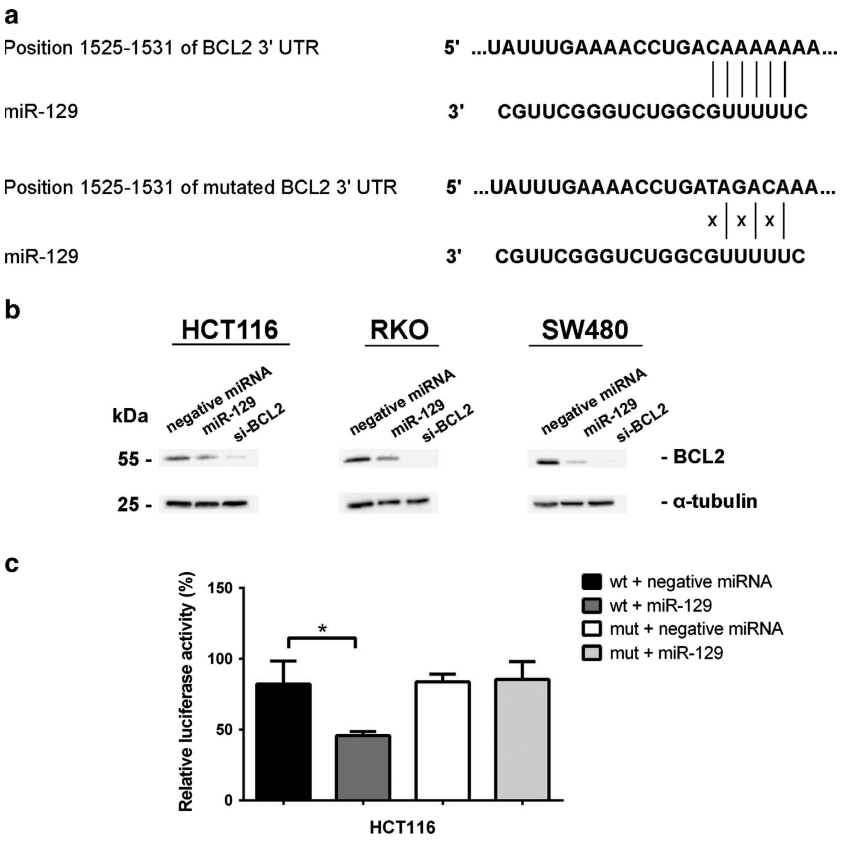

Figure 1 BCL2 is the direct target of miR-129. (**a**) A putative miR-129-binding site exists in the 3′-UTR of BCL2 mRNA and three point mutations were generated in the binding site. (**b**) Ectopic expression of miR-129 or siBCL2 in HCT116, RKO and SW480 cells decreased BCL2 protein levels by western immunoblot analysis. (**c**) Transfection of miR-129 inhibited firefly luciferase activity of pMIR-REPORT-3′-UTR-BCL2 (wild-type, wt) and such inhibition was absent with mutations in the miR-129-binding site (mutant, mut). The impact of miR-129 on BCL2 expression was normalized and compared with the negative miRNA ($n=3$, $P<0.05$)

We reasoned that defects in miRNA-mediated apoptotic pathways would contribute to 5-FU-based chemotherapy. MicroRNA-129 (miR-129) was predicted to interact with the 3′-UTR of BCL2 mRNA by TargetScan and RNAhybrid algorithms. The expression of miR-129 has been reported to be downregulated in CRC because of hypermethylation of its promoter.[26] However, the functional significance of miR-129 in CRC remains elusive. In this study, we identified a novel mechanism of direct regulation of BCL2 expression by miR-129, leading to the activation of the intrinsic apoptosis pathway. In addition, we also showed that miR-129 suppressed the expression of 5-FU protein target TS and cell-cycle control protein E2F3. Ectopic expression of miR-129 promoted apoptosis, inhibited cell growth and caused cell-cycle arrest in CRC cells. The expression of miR-129 was significantly downregulated in CRC tissue specimens compared with the paired normal control tissues. More importantly, we demonstrated that miR-129 sensitized CRC cells to 5-FU both *in vitro* and *in vivo*.

Results

BCL2 is a direct target of miR-129 in CRC cells. BCL2 is a critical molecule for the regulation of apoptosis.[27] We have identified a putative miR-129-binding site at positions 1525–1531 (CAAAAA) in the 3′-UTR of BCL2 mRNA using TargetScan and RNAhybrid algorithms (Figure 1a). To experimentally demonstrate that the expression of BCL2 is controlled by miR-129, we transfected three CRC cell lines, HCT116, RKO and SW480 with either negative control miRNA or miR-129 and quantified the protein expression of BCL2 by western immunoblot analysis. siRNA against BCL2 (siBCL2) was used as a positive control. Our results revealed that miR-129 reduced the BCL2 protein expression in all cell lines tested compared with the negative control miRNA (Figure 1b). To further confirm the direct interaction between miR-129 and BCL2 mRNA, we cloned the predicted miR-129-binding site from BCL2 mRNA into a luciferase reporter vector (Figure 1a). We co-transfected the cloned plasmid with either negative control miRNA or miR-129 into HCT116 cells, and measured the luciferase activity. We observed that miR-129 significantly inhibited the luciferase activity compared with the negative control miRNA (Figure 1c), suggesting that miR-129 was able to interact directly with the 3′-UTR of BCL2 mRNA. In addition, miR-129 did not inhibit the luciferase activity of the reporter vector containing 3′-UTR of BCL2 with three point mutations in the miR-129-binding site (Figures 1a and c). Based on these results, we conclude that miR-129 specifically suppresses BCL2 protein synthesis in CRC cells.

To fully understand the impact of miR-129 on apoptotic and other cell death pathways, we quantified 84 genes involved in cell death pathways via real-time qRT-PCR analysis comparing

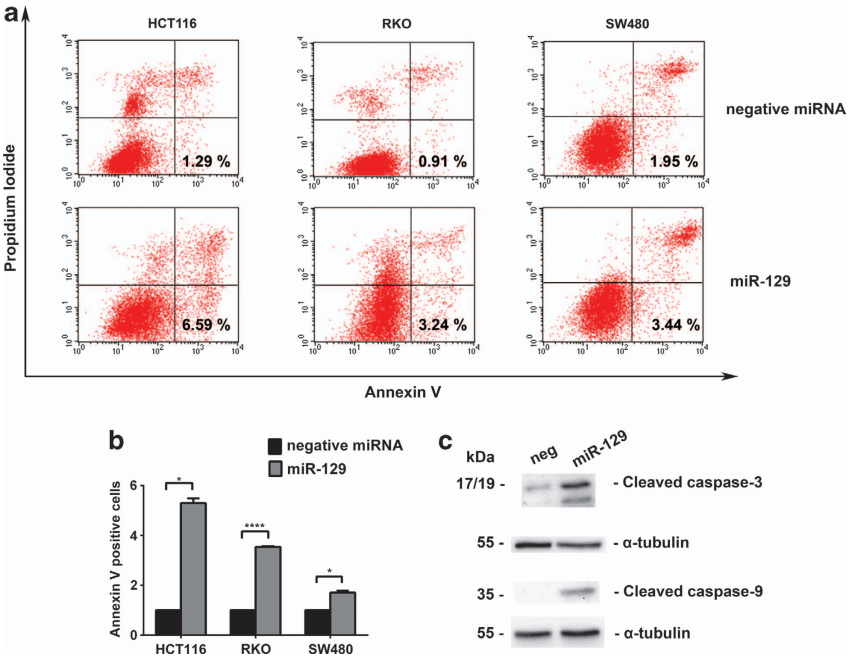

Figure 2 miR-129 positively regulates apoptosis. (**a**) HCT116, RKO and SW480 cells were transfected with either miR-129 or negative miRNA, and stained with annexin V and propidium iodide (PI) after 48 h. The representative apoptosis pattern was shown and, the apoptotic cells (annexin V positive, PI negative) were indicated as the percentage of gated cells. Quantitative analysis of apoptosis was shown in (**b**). (**c**) Western immunoblot analysis was performed for cleaved caspase-3 and cleaved caspase-9 in HCT116 cells with ectopic expression of miR-129 ($n = 3$)

miR-129-transfected cells with negative miRNA-transfected control cells. Our results indicated a significant downregulation in BCL2 mRNA expression levels, which is consistent with our western immunoblot analysis. Moreover, we observed significant differences in other apoptosis-related targets, particularly the ones acting in the intrinsic apoptosis pathway (Table 1). These data suggest that miR-129 has a major role in the regulation of apoptosis by directly targeting BCL2 as well as by impacting other critical cell death-related proteins.

miR-129 promotes apoptosis in CRC cells. BCL2 is an antiapoptotic gene involved in an evolutionarily conserved intrinsic apoptosis pathway. It acts by blocking the release of cytochrome c from mitochondria and inhibiting the activation of caspase 9, and subsequently caspase 3.[28] To identify the biological effects of BCL2 repression by miR-129, we performed a FACS analysis to quantify apoptosis via annexin V and propidium iodide staining. Our results showed that miR-129 increased apoptosis significantly in all CRC cell lines tested, as assessed by the proportion of cells that are annexin V positive and propidium iodide negative (Figures 2a and b). To determine that such increase in apoptosis is due to the activation of the intrinsic apoptosis pathway, we quantified the protein expression of cleaved caspase-9 and cleaved caspase-3 by western immunoblot analysis. As expected, miR-129 elevated the protein levels of both cleaved caspase-9 and caspase-3 (Figure 2c). These data indicate that miR-129 functions as a pro-apoptotic molecule by directly targeting BCL2.

Overexpression of miR-129 inhibits CRC cell growth *in vitro*. The impact of miR-129 on cell proliferation and cell cycle was analyzed by comparing miR-129-transfected CRC cells with negative miRNA-transfected control cells. Cell proliferation was significantly inhibited with miR-129 transfection (Figure 3a). At day 5, the cell proliferation of miR-129-transfected HCT116, RKO and SW480 cells were reduced by 73.9, 53.9 and 52.4% of the negative controls, respectively. We observed that the overexpression of miR-129 triggered cell-cycle arrest in both G1 and/or G2 phase (Figure 3b). G1/S and G2/S ratios indicated that the cell-cycle arrest reached significance at G2 checkpoint in HCT116 cells, and at G1 checkpoint in RKO cells (Figure 3c). These results reveal that miR-129 inhibits cell proliferation and induces cell-cycle arrest in CRC cells.

Table 1 miR-129 regulated targets that are related to apoptosis

Gene symbol	Gene title	Fold change (miR-129/neg)
BCL2	B-cell CLL/lymphoma 2	0.006
BCL2A1	BCL2-related protein A1	0.04
BIRC3	Baculoviral IAP repeat containing 3	0.28
PARP2	Poly (ADP-ribose) polymerase 2	0.47
APAF1	Apoptotic peptidase activating factor 1	2.44
BAX	BCL2-associated X protein	27.77
CASP2	Caspase 2, apoptosis-related cysteine peptidase	7.68
CASP3	Caspase 3, apoptosis-related cysteine peptidase	1.27
CASP7	Caspase 7, apoptosis-related cysteine peptidase	4.75
CASP9	Caspase 9, apoptosis-related cysteine peptidase	2.53
MCL1	Myeloid cell leukemia sequence 1 (BCL2 related)	3.81

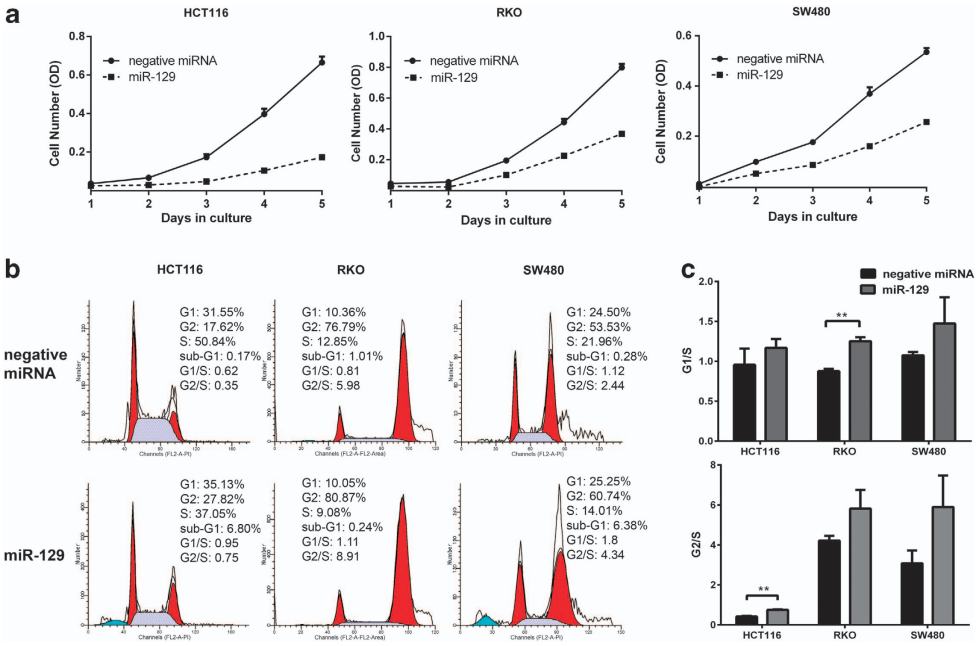

Figure 3 miR-129 suppresses CRC cell growth and induces cell-cycle arrest. (**a**) HCT116, RKO and SW480 cells were transfected with either miR-129 or negative miRNA, and cell numbers were measured with WST-1 assay. Cell-cycle analysis was performed to determine the impact of miR-129. The representative flow cytometry pattern was shown in (**b**) and the G1/S and G2/S ratios were shown in (**c**) ($n = 3$)

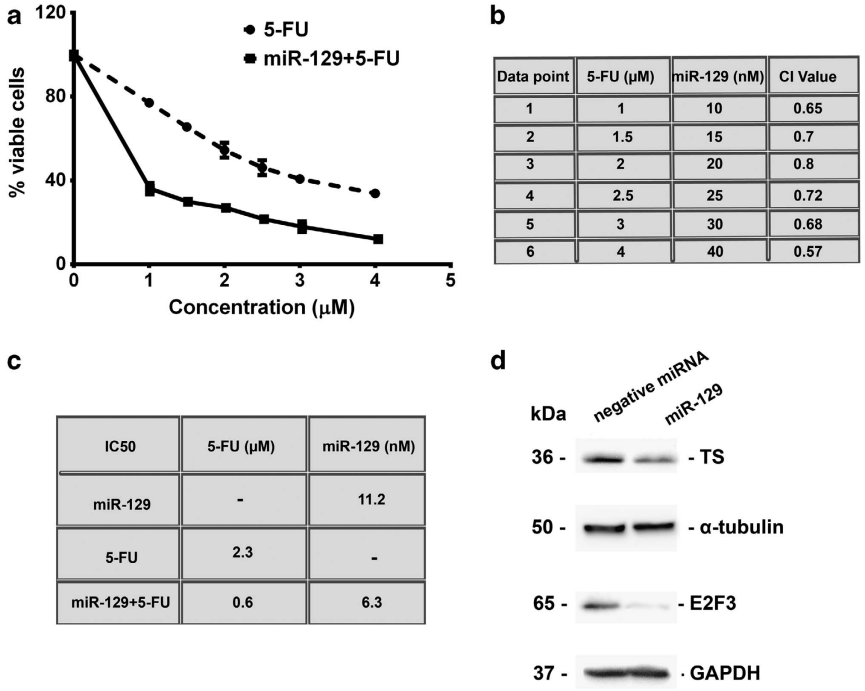

Data point	5-FU (μM)	miR-129 (nM)	CI Value
1	1	10	0.65
2	1.5	15	0.7
3	2	20	0.8
4	2.5	25	0.72
5	3	30	0.68
6	4	40	0.57

IC50	5-FU (μM)	miR-129 (nM)
miR-129	-	11.2
5-FU	2.3	-
miR-129+5-FU	0.6	6.3

Figure 4 miR-129 functions synergistically with 5-FU *in vitro*. (**a**) The inhibitory effects of 5-FU on the growth of HCT116 cells alone or in combination with miR-129 were observed by WST-1 assay. (**b**) The combination effects of 5-FU and miR-129 were determined by calculating the CI values for each data point in (**a**). CI < 1 indicates a synergistic effect. (**c**) IC_{50} values were determined based on the 50% growth inhibition using WST-1 assay. (**d**) Western immunoblot analysis was performed for TS and E2F3 protein levels in HCT116 cells with ectopic expression of miR-129

miR-129 enhances 5-FU cytotoxicity *in vitro*. On the basis of the profound effect of miR-129 on proliferation and apoptosis, we tested the impact of miR-129 on the most widely used chemotherapy drug in CRC, 5-FU. We treated HCT116 cells with either precursor miR-129 or 5-FU or miR-129 and 5-FU combination (at a fixed ratio 1 : 10) for 72 h. Then, we constructed a concentration-dependent curve based on the cell viability of cells treated with 5-FU alone

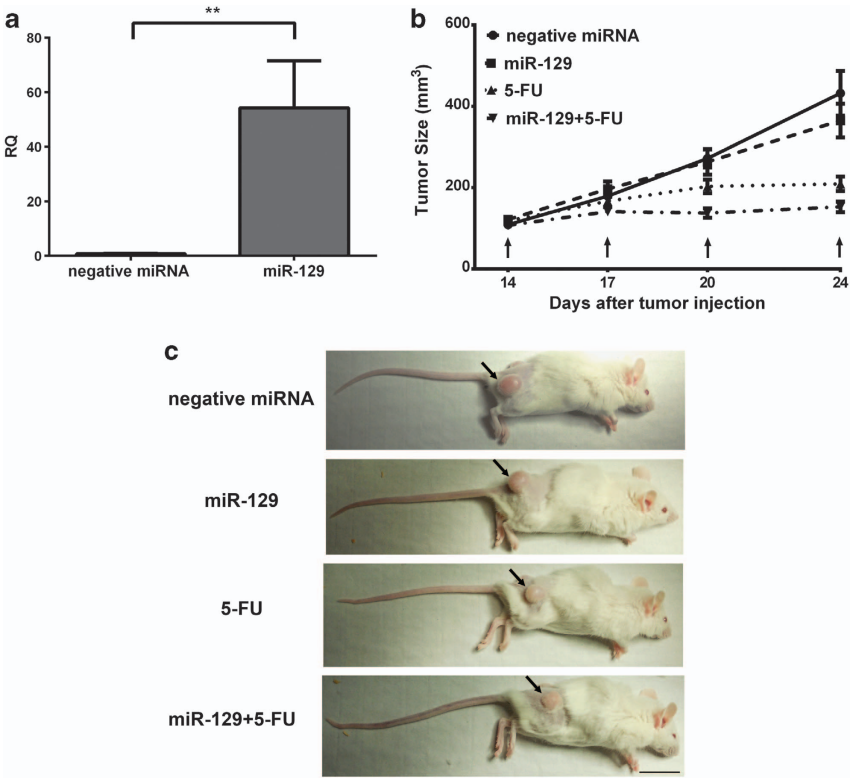

Figure 5 miR-129 enhances 5-FU cytotoxicity *in vivo*. (**a**) Expression level of miR-129 in tumor xenografts was quantified by real-time qRT-PCR and miR-129 injected tumors had significantly higher levels of miR-129 than the negative controls ($n=3$, $P<0.01$). (**b**) HCT116 cells were subcutaneously injected into NOD/SCID mice. On days 14, 17 and 20 (indicated by arrows), mice were treated with either negative miRNA ($n=6$) or miR-129 precursor ($n=5$) or 5-FU alone ($n=5$) or 5-FU and miR-129 together ($n=5$), and tumor sizes were measured during the treatment until day 24 when mice were killed. (**c**) Representative images of mice bearing HCT116 tumors at day 24 were shown. Arrows indicate the subcutaneous tumors. Scale bar: 2 cm

or with miR-129 and 5-FU combination. The graph demonstrated a significant increase in cell death in the combined treatment compared with 5-FU treatment alone (Figure 4a). To determine whether combination of miR-129 with 5-FU had any synergy, we calculated the combination index (CI) for each combination treatment in Figure 4a.[29,30] $CI<1$, $CI=1$ and $CI>1$ indicate synergistic, additive and antagonistic effects, respectively.[31] Our data showed the CI values were <1 in all combinations tested (Figure 4b). Finally, the effect of combination on IC_{50} values was illustrated in Figure 4c. The IC_{50} values for miR-129 and 5-FU were 11.2 nM and 2.3 μM, respectively. When combined, IC_{50} values for miR-129 and 5-FU decreased to 6.3 nM and 0.6 μM, respectively. Taken together, these results suggest that miR-129 exerts a strong synergistic effect with 5-FU on the growth of CRC cells.

The main mechanism of action of 5-FU is through inhibition of a critical target in cellular proliferation, TS.[5] Based on the finding that miR-129 functioned cooperatively with 5-FU, we further investigated the effect of miR-129 on TS protein levels. Of note, TS is also one of the predicted targets of miR-129 based on the TargetScan analysis. Our results revealed that miR-129 suppressed the protein expression of TS, providing an explanation for the synergy of 5-FU with miR-129 (Figure 4d). Moreover, a study by Akao *et al.*[32] described the role of a miRNA, miR-34a, in the modulation of 5-FU chemoresistance in human CRC cells by targeting E2F3. E2F3 is a transcription factor that regulates cell-cycle progression,[33] and it has been reported to be a potential target of miR-129 based on a microarray analysis.[34] The E2F3 protein expression was quantified after miR-129 transfection by western immunoblot analysis. Our results revealed that miR-129 was able to reduce E2F3 protein levels (Figure 4d). Therefore, we conclude that miR-129 acts on several critical genes regulating apoptosis, proliferation and cell cycle, which leads to an anti-proliferative and apoptotic phenotype, and ultimately enhanced chemosensitivity.

miR-129 enhances 5-FU cytotoxicity *in vivo*. To demonstrate the proof-of-principle that delivering miR-129 *in vivo* could potentially increase the cytotoxic effect of 5-FU, we established a mouse colorectal tumor xenograft model by subcutaneously inoculating 2.5×10^6 HCT116 cells (with 50% matrigel) in NOD/SCID mice. When solid and palpable tumors with an average volume of 100–150 mm^3 were formed (at day 14), we randomly separated mice into four groups such that each group was treated either with negative control miRNA, miR-129 alone, 5-FU alone or miR-129 and 5-FU together. The miRNAs were complexed with siPORTamine and injected intratumorally while 5-FU (50 μg/g) was injected via the tail vein. All injections were applied at 3-day intervals for a total of three times before the tumors were collected at day 24. Of note, we only used unmodified synthetic miRNAs, and quantified the expression levels of

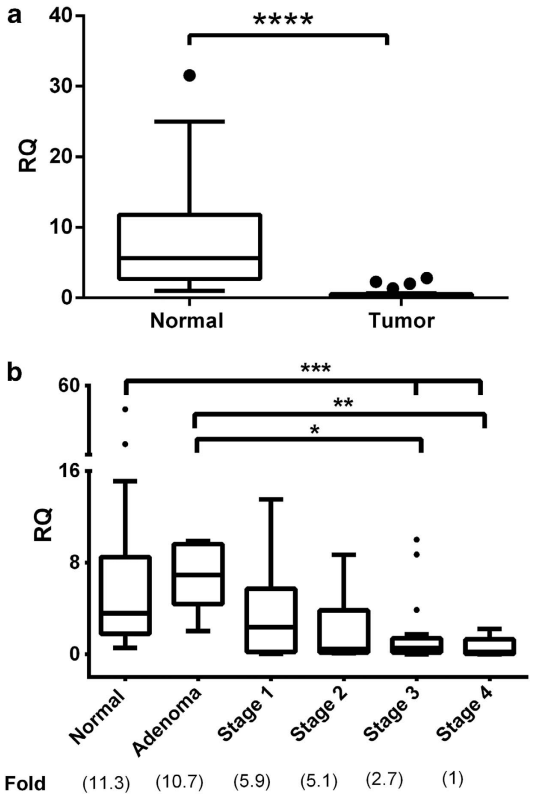

Figure 6 miR-129 is downregulated in CRC clinical samples. (**a**) Expression level of miR-129 was quantified by real-time qRT-PCR in paired tumor and normal tissues from CRC patients, and normalized to the internal control RNU44. Statistical significance was calculated by Wilcoxon matched-pairs signed-rank test ($P<0.0001$). (**b**) Expression of miR-129 in normal, adenoma and tumor tissues from different stages of CRC was demonstrated. Statistical significance was calculated by Kruskal–Wallis one-way analysis of variance test ($P<0.0001$) with Dunn's multiple comparisons test

miR-129 in tumor xenografts after killing by real-time qRT-PCR analysis. We found that miR-129 injected tumors had approximately 69-fold increase in miR-129 levels compared with negative control group (Figure 5a), suggesting that delivery of miR-129 into the tumors was successful. Importantly, despite the overexpression, the expression levels of miR-129 remained at a rather low copy number within the physiological range (<20 copies per cell based on cycle threshold value at 30, which is equal to the expression of miR-129 in normal colon mucosa) as the control tumor xenografts had virtually no miR-129 expression (cycle threshold value at 35). Our results showed that miR-129 treatment alone was able to reduce the tumor size even at this low expression level, and, as expected, 5-FU treatment alone induced a strong inhibitory effect ($P<0.01$, at day 24) compared with negative miRNA. However, more importantly, when miR-129 was combined with 5-FU, it caused greater inhibition of tumor growth than 5-FU treatment alone ($P<0.001$, at day 24). The average volume of miR-129 treated, 5-FU treated or miR-129 and 5-FU treated tumors were reduced by $\sim$15.6, 51.6 and 64.6% of the control group at day 24, respectively(Figure 5b). Images of tumor-bearing mice at day 24 were also shown in Figure 5c. Taken together, these results provide novel evidence that miR-129 can enhance the effectiveness of 5-FU on tumor growth *in vivo*.

miR-129 is downregulated in human colorectal tumor tissues. To directly demonstrate the clinical significance of miR-129, we profiled the expression levels of miR-129 from 22 paired fresh-frozen human colorectal tumor tissues and normal controls using real-time qRT-PCR analysis. The expression of miR-129 was significantly decreased in tumor tissues compared with normal controls ($P<0.0001$; Figure 6a). To evaluate the impact of miR-129 in CRC progression, we further profiled the expression of miR-129 from another set of 61 archival formalin-fixed paraffin-embedded (FFPE) colorectal specimens. The levels of miR-129 in CRC patients with different stages of the disease were presented in Figure 6b. Our results showed that the expression of miR-129 was significantly reduced in patients with stage 3 and stage 4 of the disease compared with the normal or adenoma tissues; whereas this reduction was absent in patients with stage 1 and stage 2 CRC. Based on these results, we suggest that the decreased levels of miR-129 may be associated with the progression of CRC and may open a new avenue for therapeutic intervention in CRC patients.

On the basis of our results, a model was proposed for the potential roles of miR-129 in CRC (Figure 7). miR-129 promotes apoptosis via the suppression of BCL2. miR-129 suppresses the protein expression of TS and E2F3, which impact cellular proliferation and cell cycle. In the end, increased apoptosis, decreased proliferation and cell-cycle arrest cause an inhibitory effect on the growth of tumor cells and thereby leads to enhanced chemosensitivity. Additional targets mediated by miR-129 may also contribute to this model.

Discussion

In this study, we identified a novel regulatory mechanism of BCL2 gene expression mediated by miR-129 in CRC. More importantly, the suppression of BCL2 as well as other important targets such as TS and E2F3 acted in concert to trigger CRC cell apoptosis, cell-cycle arrest and inhibition of cell proliferation. As a result, miR-129 sensitized CRC cells to 5-FU treatment both *in vitro* and *in vivo* mice tumor xenografts. Resistance to 5-FU treatment is one of the major causes for the failure of chemotherapy in treating advanced CRC.[5] Therefore, it is critical to discover new strategies to increase the effectiveness of 5-FU for therapeutic purposes. miR-129 expression was prominently and progressively reduced in CRC patient specimens. There was no significant difference in miR-129 expression between normal/adenoma and stage 1/stage 2 cancers. However, miR-129 levels were dramatically decreased in stage 3 and stage 4 cancers (Figures 6a and b). These results show that loss of miR-129 expression is significantly correlated with the progression of CRC. This is consistent with a previous report that abnormal hypermethylation of the promoter of hsa-miR-129 is associated with reduced expression in CRC tissues but rare in normal tissue.[26] Our data, in addition, provided novel molecular and cellular mechanisms of miR-129 and its potential clinical significance in cancer progression.

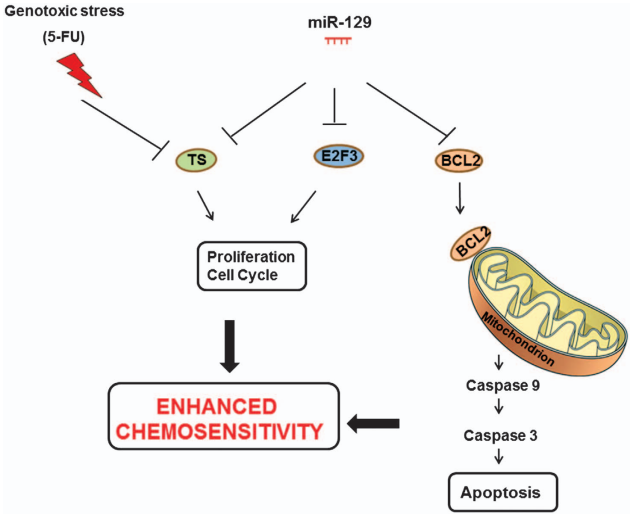

Figure 7 Proposed model of miR-129 function as a potential tumor suppressor in CRC and a sensitizer to 5-FU-based chemotherapy. miR-129 suppresses the protein expression of three critical targets, BCL2, TS, and E2F3. Downregulation of BCL2 activates the intrinsic apoptosis pathway by cleaving caspase-9 and caspase-3. Downregulation of TS and E2F3 inhibits cell proliferation by impacting cell cycle. Thereby, miR-129 exerts a strong antitumor phenotype by induction of apoptosis and impairment of proliferation in tumor cells. Ultimately, this phenotype sensitizes CRC cells to fluoropyrimidine-based chemotherapy

Moreover, downregulation of miR-129 has been observed in other tumor types such as gastric cancer, breast cancer, hepatocellular carcinoma, CRC, lung carcinoma and medulloblastoma.[35–40] Thus, we postulate that the significance of this mechanism may extend to a wide range of cancer types.

A tumor-suppressor function of miR-129 has been demonstrated in the present work, mainly acting as a pro-apoptotic miRNA by targeting BCL2. There are also a number of miRNAs reported to suppress BCL2 in various tumor types.[41–43] Such redundancy may indicate the existence of a unique mechanism to regulate BCL2, dependent on the cell type and cellular context. It is clear that, in CRC, miR-129 is the main contributor to suppress BCL2 expression. It is worth pointing out that miR-129 also suppressed the expression of 5-FU target protein TS. As a result, it creates another level of synergy, in addition to triggering apoptosis by knocking down BCL2, to enhance chemosensitivity to 5-FU. This phenotype is opposite to that of miR-215, which we previously reported, suppressed TS protein expression, however, counterintuitively caused chemoresistance to 5-FU. This was probably because miR-215 did not trigger any type of cell death but induced cell-cycle arrest by inhibiting DTL (denticleless protein homolog), a key E3 ubiquitin ligase,[10] as it is well known that DNA-damaging agents such as 5-FU are effective for only rapidly proliferating tumor cells. Therefore, the ability of miR-129 to trigger apoptosis is quite significant in this regard. E2F3 suppressed by miR-129 is also contributing to the enhanced chemosensitivity, because it has previously been demonstrated that upregulation of E2F family proteins contributes to 5-FU resistance.[44]

BCL2 is a central anti-apoptotic protein, and blockade of BCL2 activity has been considered as a novel therapeutic strategy for a wide variety of cancers.[45–51] The data presented in this study are of considerable therapeutic significance because miR-129 not only suppressed BCL2, but it also had a broader tumor-suppressive impact by regulating other critical targets. miR-129-based therapeutics could help to achieve the multi-targeted anticancer therapeutic strategy. As 5-FU-based chemotherapy is still the main treatment option for advanced metastatic CRC, it is important that a miR-129 restoration approach may offer a new modulation strategy to overcome chemoresistance. Importantly, in our *in vivo* tumor xenografts, we have shown that by increasing miR-129 expression to normal levels using only unmodified synthetic miRNAs, tumors became more sensitive to 5-FU. We believe that this impact may further be improved by chemical modifications of miR-129 or optimized delivery systems.[52]

In summary, our results reveal that miR-129 promotes apoptosis by suppressing BCL2 protein expression in CRC. Furthermore, miR-129 induces cell-cycle arrest and inhibition of cell proliferation, and enhances 5-FU cytotoxicity *in vitro* and *in vivo*. Restoration of miR-129 levels could be a future direction to develop a novel therapeutic strategy to modulate and to enhance chemosensitivity to 5-FU treatment.

Materials and Methods

Cell culture. The human CRC cell line HCT116 was kindly provided by Professor Bert Vogelstein (The Johns Hopkins University, Baltimore, MD, USA), and maintained in McCoy's 5A medium (Gibco Laboratories, Frederick, MD, USA). The other human CRC cell lines RKO and SW480 were purchased from the American Type Culture Collection (ATCC, Manassas, VA, USA), and were maintained in DMEM medium (Gibco Laboratories). All media were supplemented with 10% fetal bovine serum (Sigma-Aldrich, St. Louis, MO, USA).

Patient samples. Two clinical sample cohorts were used for this study approved by the institution review board. Patient consent forms were obtained from each patient according to institutional policies. The first cohort consisted of 22 CRC patients who underwent surgical resection of primary tumors at the Department of Visceral and Transplantation Surgery, University of Ulm, Germany. Each patient sample contained a pair of snap-frozen specimens from normal colorectal mucosa and tumor. The second cohort consisted of 55 patients with primary CRC who underwent surgery at the Stony Brook University Hospital, Stony Brook, NY, USA. FFPE tissues (21 normal, 9 stage 1, 9 stage 2, 14 stage 3 and 2 stage 4) were acquired from the archival collections of the Department of Pathology.

miRNA and siRNA transfection. HCT116, RKO and SW480 cells were plated in six-well plates at 2×10^5, 1×10^5 and 1×10^5 per well, respectively. Twenty-four hours after plating, 100 nM of miR-129 precursor (Ambion, Carlsbad, CA, USA) or siBCL2 (Dharmacon, Lafayette, CO, USA) were transfected to the cells with oligofectamine (Invitrogen, Carlsbad, CA, USA) in accordance with the manufacturer's protocol. Negative miRNA (Ambion) was also transfected as a negative control.

Western immunoblot analysis. Forty-eight hours after transfection, cells were lysed with RIPA buffer (Sigma-Aldrich), and western immunoblotting was performed using standard procedures. The primary antibodies used for the analysis were mouse anti-human BCL2 antibody (1 : 200; Thermo Fisher Scientific, Fremont, CA, USA), rabbit anti-human cleaved caspase-3 antibody (1 : 200; Cell Signaling Technology, Beverly, MA, USA), rabbit anti-human cleaved caspase-9 antibody (1 : 200; Cell Signaling Technology), mouse anti-human E2F3 antibody (1 : 5000; Millipore, Billerica, MA, USA), mouse anti-human TS antibody (1 : 400; Millipore), mouse anti-human GAPDH antibody (1 : 1000, Santa Cruz Biotechnology, Santa Cruz, CA, USA) or mouse anti-human α-tubulin antibody (1 : 1000; Millipore). Horseradish peroxidase-conjugated (HRP) antibodies against mouse (1 : 5000; Bio-Rad, Hercules, CA, USA) or against rabbit (1 : 5000; Cell Signaling Technology) were used as the secondary antibodies. HRP activity was detected

with SuperSignal West Pico Chemiluminescent Substrate (Thermo Fisher Scientific) and visualized in an UVP Bioimaging system (Upland, CA, USA).

Luciferase assay. The predicted miR-129-binding sequence (wild-type, underlined) or a mismatch sequence (mutant, italic underlined) in the 3′-UTR of BCL2 mRNA were synthesized with *Spe*I and *Pme*I restriction site overhangs (Invitrogen). After annealing, double-strand oligonucleotides were inserted into the pMIR-REPORT plasmid (Invitrogen), downstream of the firefly luciferase reporter. The sequences of these synthesized oligonucleotides are: forward wild-type: 5′-CTAGTTCACTGTAGTTTGGTTTTATTTGAAAACCTGACAAAAAAAAAGTTCCAG GT-3′; reverse wild-type: 5′-AAACACCTGGAACTTTTTTTTTGTCAGGTTTT CAAATAAAAC-CAAACTACAGTGA-3′; forward mutant: 5′-CTAGTTCACTG TAGTTTGGTTTTATTTGAAAACCTGA*TAGACA*AAAAAGTTCCAGGT-3′; reverse mutant: 5′-AAACACCTGGAACTTTTTGTCTATCAGGTTTTCAAATAAAACCAAAC TACAGTGA-3′.

Twenty-four hours before transfection, 1.5×10^4 cells were plated in 96-well plate. In all, 10 nM of miR-129 or negative miRNA was transfected into cells together with 100 ng of pMIR-REPORT-3′-UTR-BCL2 (wild-type or mutant) and 1 ng of Renilla luciferase plasmid pRL-SV40 (Promega, Madison, WI, USA) by DharmaFect Duo (Dharmacon) following the manufacturer's protocol. Luciferase assay was performed 24 h after transfection by dual-luciferase reporter assay system (Promega). For each sample, firefly luciferase activity was normalized to Renilla luciferase activity and the inhibition by miR-129 was normalized to the control miRNA.

Cell death pathwayfinder PCR array. RNAs were extracted from cells transfected with either precursor miR-129 or negative miRNA using TRIzol reagent (Invitrogen) in accordance with the manufacturer's protocol. RNAs were transcribed to first-strand cDNA using the RT^2 First Strand Kit (SABiosciences, Qiagen, Venlo, The Netherlands). Next, the cDNA is mixed with RT^2 SYBR Green Mastermix (SABiosciences), and this mixture is aliquoted into the wells of the Cell Death PathwayFinder PCR Array (PAHS-212Z). Applied Biosystems 7500 Real-Time PCR machine was used for qRT-PCR (Applied Biosystems, Foster City, CA, USA), and relative expression values were determined using the ΔΔCT method.

Apoptosis assay. Forty-eight hours after transfection, cells were harvested, stained with propidium iodide and anti-annexin-V antibody (Annexin V-FITC Apoptosis Detection kit, BD Biosciences, San Jose, CA, USA) following the manufacturer's protocol, and stained cells were detected by flow cytometry. The experiments for the apoptosis assay were performed at least three times.

Cell proliferation assay. Twenty-four hours after transfection, cells were seeded in 96-well plates at a density of 2000 cells per well. The cell proliferation assay was performed on days 1, 3 and 5 by incubating 10 μl WST-1 (Roche Applied Science, Mannheim, Germany) in the culture medium for 1 h and reading the absorbance at 450 and 630 nm. The cell proliferation rate was calculated by subtracting the absorbance at 450 nm from the absorbance at 630 nm. Experiments for the cell proliferation assay were performed at least three times.

Cell-cycle analysis. Thirty-six hours after transfection, cells were harvested and resuspended at 0.5 to 1×10^6 cells/ml in modified Krishan buffer supplemented with 0.02 mg/ml RNase H (Invitrogen) and 0.05 mg/ml propidium iodide (Sigma-Aldrich).[53] Stained cells were detected by flow cytometry and results were analyzed with Modfit LT software. The experiments for cell-cycle analysis were performed at least three times.

5-FU treatment and cytotoxicity assay. Twenty-four hours after transfection, HCT116 cells were plated in 96-well plates at 2×10^3 cells per well in triplicates in 100 μl of medium. After 24 h, fresh medium containing 5-FU alone (ranged from 1 to 4 μM) or miR-129 precursor alone (ranged from 10 to 40 nM) or 5-FU and miR-129 together (at a constant ratio 1 : 10, with increasing concentrations of both compounds) were added, and cells were cultured for an additional 72 h. Cell viability was measured using the WST-1 assay, and concentration-dependent curves were generated based on the cell viability. The CI was calculated by CompuSyn software (www.combosyn.com).[30]

CRC xenografts. In all, 10- to 12-week-old NOD/SCID mice (Jackson Laboratories, Bar Harbor, MA, USA) were used for tumor implantation. All animal procedures were approved by the Stony Brook University Institutional Animal Care and Use Committee. The tumor implantation and miRNA injection protocol was modified from Trang *et al.*[54] The mice were anesthetized by isoflurane inhalation. HCT116 cells were subcutaneously injected into the lower back areas of the mice using 2.5×10^6 cells in 100 μl McCoy's 5A with 50% matrigel (BD Biosciences). The tumor size was measured using a caliper and tumor volume was calculated using the formula $V = \text{length} \times \text{width}^2/2$. When tumor volumes reached 100–150 mm^3 at day 14 post-injection, the mice were randomly assigned into four groups. For the first two groups, 10 μM negative miRNA or miR-129 precursor (Ambion) complexed with 1.6 μl siPORTAmine (Ambion) in 50 μl McCoy's 5A was injected into the tumors every 3 days. For the third group, 5-FU (Sigma-Aldrich) was injected at 50 μg/g via the tail vein every 3 days. Finally, for the last group, both miR-129 precursor and 5-FU were injected as described above. The mice were killed on day 24 post-injection by CO_2 inhalation, and tumors were dissected out for RNA isolation.

RNA isolation. For mouse xenografts, sectioned tissues were deparaffinized, hydrated and digested with proteinase K (Sigma-Aldrich) respectively. Subsequently, total RNA was isolated using the TRIzol reagent (Invitrogen). Total RNA was also isolated from clinical specimens by the TRIzol-based approach.

Real-time qRT-PCR analysis of miR-129 expression. The miR-129-specific primer and the internal control RNU44 gene were purchased from Ambion. cDNA synthesis was performed by the High Capacity cDNA Synthesis Kit (Applied Biosystems) with miRNA-specific primers. Real-time qRT-PCR was carried out on an Applied Biosystems 7500 Real-Time PCR machine with miRNA-specific primers by TaqMan Gene Expression Assay (Applied Biosystems). Expression level of miR-129 was calculated by the ΔΔCT method based on the internal control RNU44, normalized to the control group and plotted as relative quantification.

Statistical analysis. All statistical analyses were performed with Graphpad Prism (version 6.01) software (La Jolla, CA, USA). The statistical significance between two groups was determined by Wilcoxon matched-pairs signed-rank test for clinical samples and by Student's unpaired *t*-test for all other experiments. The statistical significance among several groups was analyzed by Kruskal–Wallis one-way analysis of variance test with Dunn's multiple comparisons test. Data were expressed as mean ± S.E.M. The statistical significance is either described in figure legends, or indicated with asterisks (*). $*P<0.05$; $**P<0.01$; $***P<0.001$; $****P<0.0001$.

Conflict of Interest

The authors declare no conflict of interest.

Acknowledgements. We appreciate the critical reviews by Mr. Andrew Fesler. This study was supported by R01CA155019 (J Ju) and R33CA147966 (J Ju).

1. Siegel R, Naishadham D, Jemal A. Cancer statistics, 2013. *Cancer J Clin* 2013; **63**: 11–30.
2. Meyerhardt JA, Mayer RJ. Systemic therapy for colorectal cancer. *N Engl J Med* 2005; **352**: 476–487.
3. Danenberg PV. Thymidylate synthetase - a target enzyme in cancer chemotherapy. *Biochimica et Biophysica Acta* 1977; **473**: 73–92.
4. Chu E, Callender MA, Farrell MP, Schmitz JC. Thymidylate synthase inhibitors as anticancer agents: from bench to bedside. *Cancer Chemother Pharmacol* 2003; **52** (Suppl 1): S80–S89.
5. Longley DB, Johnston PG. 5-Fluorouracil. *Apoptosis Cell Signaling Human Diseases* 2007; **1**: 263–278.
6. Gottesman MM, Fojo T, Bates SE. Multidrug resistance in cancer: role of ATP-dependent transporters. *Nat Rev Cancer* 2002; **2**: 48–58.
7. Silvera D, Formenti SC, Schneider RJ. Translational control in cancer. *Nat Rev Cancer* 2010; **10**: 254–266.
8. Ma J, Dong C, Ji C. MicroRNA and drug resistance. *Cancer Gene Ther* 2010; **17**: 523–531.
9. Sarkar FH, Li Y, Wang Z, Kong D, Ali S. Implication of microRNAs in drug resistance for designing novel cancer therapy. *Drug Resistance Updates Rev Commentaries Antimicrobial Anticancer Chemother* 2010; **13**: 57–66.
10. Song B, Wang Y, Titmus MA, Botchkina G, Formentini A, Kornmann M *et al.* Molecular mechanism of chemoresistance by miR-215 in osteosarcoma and colon cancer cells. *Mol Cancer* 2010; **9**: 96.
11. Fu L, Minden MD, Benchimol S. Translational regulation of human p53 gene expression. *EMBO J* 1996; **15**: 4392–4401.

12. Chu E, Koeller DM, Casey JL, Drake JC, Chabner BA, Elwood PC *et al.* Autoregulation of human thymidylate synthase messenger RNA translation by thymidylate synthase. *Proc Natl Acad Sci USA* 1991; **88**: 8977–8981.
13. Allen KE, Weiss GJ. Resistance may not be futile: microRNA biomarkers for chemoresistance and potential therapeutics. *Mol Cancer Therapeutics* 2010; **9**: 3126–3136.
14. Song B, Ju J. Impact of miRNAs in gastrointestinal cancer diagnosis and prognosis. *Expert Rev Mol Med* 2010; **12**: e33.
15. Lee RC, Feinbaum RL, Ambros V. The C. elegans heterochronic gene lin-4 encodes small RNAs with antisense complementarity to lin-14. *Cell* 1993; **75**: 843–854.
16. Bartel DP. MicroRNAs: genomics, biogenesis, mechanism, and function. *Cell* 2004; **116**: 281–297.
17. Bartel DP. MicroRNAs: target recognition and regulatory functions. *Cell* 2009; **136**: 215–233.
18. Lim LP, Lau NC, Garrett-Engele P, Grimson A, Schelter JM, Castle J *et al.* Microarray analysis shows that some microRNAs downregulate large numbers of target mRNAs. *Nature* 2005; **433**: 769–773.
19. Ambros V. The functions of animal microRNAs. *Nature* 2004; **431**: 350–355.
20. Brennecke J, Hipfner DR, Stark A, Russell RB, Cohen SM. Bantam encodes a developmentally regulated microRNA that controls cell proliferation and regulates the proapoptotic gene hid in Drosophila. *Cell* 2003; **113**: 25–36.
21. Calin GA, Sevignani C, Dumitru CD, Hyslop T, Noch E, Yendamuri S *et al.* Human microRNA genes are frequently located at fragile sites and genomic regions involved in cancers. *Proc Natl Acad Sci USA* 2004; **101**: 2999–3004.
22. Macfarlane LA, Murphy PR. MicroRNA: biogenesis, function and role in cancer. *Curr Genomics* 2010; **11**: 537–561.
23. Song B, Wang Y, Xi Y, Kudo K, Bruheim S, Botchkina GI *et al.* Mechanism of chemoresistance mediated by miR-140 in human osteosarcoma and colon cancer cells. *Oncogene* 2009; **28**: 4065–4074.
24. Cory S, Adams JM. The Bcl2 family: regulators of the cellular life-or-death switch. *Nat Rev Cancer* 2002; **2**: 647–656.
25. Baretton GB, Diebold J, Christoforis G, Vogt M, Muller C, Dopfer K *et al.* Apoptosis and immunohistochemical bcl-2 expression in colorectal adenomas and carcinomas. Aspects of carcinogenesis and prognostic significance. *Cancer* 1996; **77**: 255–264.
26. Bandres E, Agirre X, Bitarte N, Ramirez N, Zarate R, Roman-Gomez J *et al.* Epigenetic regulation of microRNA expression in colorectal cancer. *Int J Cancer* 2009; **125**: 2737–2743.
27. Hockenbery D, Nunez G, Milliman C, Schreiber RD, Korsmeyer SJ. Bcl-2 is an inner mitochondrial membrane protein that blocks programmed cell death. *Nature* 1990; **348**: 334–336.
28. Cory S, Huang DC, Adams JM. The Bcl-2 family: roles in cell survival and oncogenesis. *Oncogene* 2003; **22**: 8590–8607.
29. Ha J, Zhao L, Zhao Q, Yao J, Zhu BB, Lu N *et al.* Oroxylin A improves the sensitivity of HT-29 human colon cancer cells to 5-FU through modulation of the COX-2 signaling pathway. *Biochem Cell Biol* 2012; **90**: 521–531.
30. Chou T-C, Martin N. *CompuSyn Software for Drug Combinations and for General Dose-Effect Analysis, and User's Guide.* ComboSyn, Inc.: Paramus, NJ, USA, 2007.
31. Chou TC. Theoretical basis, experimental design, and computerized simulation of synergism and antagonism in drug combination studies. *Pharmacol Rev* 2006; **58**: 621–681.
32. Akao Y, Noguchi S, Iio A, Kojima K, Takagi T, Naoe T. Dysregulation of microRNA-34a expression causes drug-resistance to 5-FU in human colon cancer DLD-1 cells. *Cancer Lett* 2011; **300**: 197–204.
33. Welch C, Chen Y, Stallings RL. MicroRNA-34a functions as a potential tumor suppressor by inducing apoptosis in neuroblastoma cells. *Oncogene* 2007; **26**: 5017–5022.
34. Wu J, Qian J, Li C, Kwok L, Cheng F, Liu P *et al.* miR-129 regulates cell proliferation by downregulating Cdk6 expression. *Cell Cycle* 2010; **9**: 1809–1818.
35. Katada T, Ishiguro H, Kuwabara Y, Kimura M, Mitui A, Mori Y *et al.* microRNA expression profile in undifferentiated gastric cancer. *Int J Oncol* 2009; **34**: 537–542.
36. Wang QY, Tang J, Zhou CX, Zhao Q. [The down-regulation of miR-129 in breast cancer and its effect on breast cancer migration and motility]. *Sheng li xue bao: [Acta physiologica Sinica]* 2012; **64**: 403–411.
37. Anwar SL, Albat C, Krech T, Hasemeier B, Schipper E, Schweitzer N *et al.* Concordant hypermethylation of intergenic microRNA genes in human hepatocellular carcinoma as new diagnostic and prognostic marker. *Int J Cancer* 2013; **133**: 660–670.
38. Bandres E, Cubedo E, Agirre X, Malumbres R, Zarate R, Ramirez N *et al.* Identification by Real-time PCR of 13 mature microRNAs differentially expressed in colorectal cancer and non-tumoral tissues. *Mol Cancer* 2006; **5**: 29.
39. Seike M, Goto A, Okano T, Bowman ED, Schetter AJ, Horikawa I *et al.* MiR-21 is an EGFR-regulated anti-apoptotic factor in lung cancer in never-smokers. *Proc Natl Acad Sci USA* 2009; **106**: 12085–12090.
40. Ferretti E, De Smaele E, Po A, Di Marcotullio L, Tosi E, Espinola MS *et al.* MicroRNA profiling in human medulloblastoma. *Int J Cancer J* 2009; **124**: 568–577.
41. Cimmino A, Calin GA, Fabbri M, Iorio MV, Ferracin M, Shimizu M *et al.* miR-15 and miR-16 induce apoptosis by targeting BCL2. *Proc Natl Acad Sci USA* 2005; **102**: 13944–13949.
42. Zhang H, Li Y, Huang Q, Ren X, Hu H, Sheng H *et al.* MiR-148a promotes apoptosis by targeting Bcl-2 in colorectal cancer. *Cell Death Differ* 2011; **18**: 1702–1710.
43. Zhu W, Shan X, Wang T, Shu Y, Liu P. miR-181b modulates multidrug resistance by targeting BCL2 in human cancer cell lines. *Int J Cancer* 2010; **127**: 2520–2529.
44. Banerjee D, Schnieders B, Fu JZ, Adhikari D, Zhao SC, Bertino JR. Role of E2F-1 in chemosensitivity. *Cancer Res* 1998; **58**: 4292–4296.
45. Cotter FE, Waters J, Cunningham D. Human Bcl-2 antisense therapy for lymphomas. *Biochimica et Biophysica Acta* 1999; **1489**: 97–106.
46. Waters JS, Webb A, Cunningham D, Clarke PA, Raynaud F, di Stefano F *et al.* Phase I clinical and pharmacokinetic study of bcl-2 antisense oligonucleotide therapy in patients with non-Hodgkin's lymphoma. *J Clin Oncol* 2000; **18**: 1812–1823.
47. Mohammad R, Abubakr Y, Dan M, Aboukameel A, Chow C, Mohamed A *et al.* Bcl-2 antisense oligonucleotides are effective against systemic but not central nervous system disease in severe combined immunodeficient mice bearing human t(14;18) follicular lymphoma. *Clin Cancer Res* 2002; **8**: 1277–1283.
48. Cohen-Saidon C, Nechushtan H, Kahlon S, Livni N, Nissim A, Razin E. A novel strategy using single-chain antibody to show the importance of Bcl-2 in mast cell survival. *Blood* 2003; **102**: 2506–2512.
49. Wang JL, Zhang ZJ, Choksi S, Shan S, Lu Z, Croce CM *et al.* Cell permeable Bcl-2 binding peptides: a chemical approach to apoptosis induction in tumor cells. *Cancer Res* 2000; **60**: 1498–1502.
50. Lessene G, Czabotar PE, Colman PM. BCL-2 family antagonists for cancer therapy. *Nat Rev Drug Disc* 2008; **7**: 989–1000.
51. Bajwa N, Liao C, Nikolovska-Coleska Z. Inhibitors of the anti-apoptotic Bcl-2 proteins: a patent review. *Exp Opinion Therapeutic Patents* 2012; **22**: 37–55.
52. Park JK, Kogure T, Nuovo GJ, Jiang J, He L, Kim JH *et al.* miR-221 silencing blocks hepatocellular carcinoma and promotes survival. *Cancer Res* 2011; **71**: 7608–7616.
53. Krishan A. Rapid flow cytofluorometric analysis of mammalian cell cycle by propidium iodide staining. *J Cell Biol* 1975; **66**: 188–193.
54. Trang P, Medina PP, Wiggins JF, Ruffino L, Kelnar K, Omotola M *et al.* Regression of murine lung tumors by the let-7 microRNA. *Oncogene* 2010; **29**: 1580–1587.